

# CardiacMultiNet: Learning Model for Segmenting the Cardiac Images in Magnetic Resonance

Muthuraja M<sup>1</sup>, Rasmi A<sup>2\*</sup>, Shanmuga Priya S<sup>3</sup>, Maheswari K<sup>4</sup>,  
Nandhagopal Subramani<sup>5</sup>, Aravindhraj N<sup>1</sup>, Sherubha P<sup>6</sup>

<sup>1</sup>Department of Computer Science and Engineering, Kongu Engineering College, Perundurai, Erode, Tamil Nadu, India, <sup>2</sup>Information Science & Engineering, RR Institute of Technology, Bangalore, Karnataka, India, <sup>3</sup>Department of Computer Science and Engineering, SRM Institute Science and Technology, Tiruchirapalli, Tamil Nadu, India, <sup>4</sup>Department of CSE, CMR Technical Campus, Hyderabad, Telangana, India, <sup>5</sup>Department of Computer Science and Engineering (Artificial Intelligence and Machine Learning), K P R Institute of Engineering and Technology, Coimbatore, Tamil Nadu, India, <sup>6</sup>Department of Information Technology, Karpagam College of Engineering, Coimbatore, Tamil Nadu, India. \*Corresponding Author's Email: razmiraj123@zohomail.in

## Abstract

Pathologists can diagnose diseases more quickly and accurately due to advancements in Computer-Aided Design (CAD) systems, leading to increased focus on deep learning-based CAD models. In this research, the HealthLNK and ICIAR datasets are used for implementation. The proposed "MultiNet" architecture is based on inductive transmission for classifying different cardiac vascular types. It is designed to deliver fast and precise cardiovascular diagnostics through both binary and multi-class classification. The approach integrates traditional and deep learning models, including DenseNet201 and VGG19, for feature extraction from microscopic images. Compared to conventional methods, transfer learning improves accuracy significantly. Extracted features are combined in a fusion layer to generate a merged feature vector for classification. The proposed method achieves accuracy rates of 99% and 95% on the HealthLNK and ICIAR cardiac MR datasets, respectively. The "CardiacMultiNet" framework demonstrates reliability and suitability for deployment in healthcare institutions. It outperforms existing approaches, achieving 94.2 MCC and 99.4% F1-score. Additionally, benign prediction accuracy is 98.9%, malignancy prediction is 99% and the average precision reaches 99%, highlighting its effectiveness for clinical decision support.

**Keywords:** Computer-aided Diagnosis, Deep Learning Models, Magnetic Resonance Imaging, Multi-class Classification, Multi-net Framework.

## Introduction

According to the World Health Organization (WHO), worldwide 17.3 million deaths in 2008 were attributed to Cardio Vascular Diseases (CVD) problems which made up 30% of all fatalities. Decreasing CVD death and illness requires early therapy and diagnosis. Current revelations in technology and medical image processing technologies together with their application to health care have demonstrated for reaching this goal. A distinct nonionizing radiation method known as cardiac MRI gives a clear image of the anatomy of the CVD. Proper and computerized derivation of the anatomical data becomes especially critical and enables the creation of new medical request and therefore enhancing cardiology. The aim of Whole Heart Segmentation (WHS) is to isolate a heart's various structural components, which typically include the 4 circulation chambers, myocardium of the left

ventricle and occasionally the major artery of those features, have been of interest. Numerous clinical uses for the WHS findings were possible. Researchers used a flexible image-shaping technique to handle large differences in heart shapes, along with computer-based testing to find the best edges in medical images. Based on earlier studies, eight reference heart images (called atlases) were created using CT scans of the whole heart. These atlases were tested using data from different hospitals and imaging machines to make sure the method works well under various conditions. The accuracy of this heart segmentation approach was checked by testing it on eight manually labeled datasets, where one dataset was left out each time for validation. For MRI scans, a standard heart image was created using data from ten healthy individuals. A complete processing method was then developed to match and compare

This is an Open Access article distributed under the terms of the Creative Commons Attribution CC BY license (<http://creativecommons.org/licenses/by/4.0/>), which permits unrestricted reuse, distribution and reproduction in any medium, provided the original work is properly cited.

(Received 05<sup>th</sup> August 2025; Accepted 02<sup>nd</sup> April 2026; Published 26<sup>th</sup> April 2026)

to match and compare this standard image with new MRI scans to identify heart structures. To account for large differences caused by heart diseases, this standard heart image was tested on data from patients with nine different types of heart conditions. However, the results showed that using just one standard image was not better than using multiple reference images.

Recent advances in medical image segmentation have been propelled by fast developments in the deep learning and neural architecture development, especially in cardiovascular and multimodal image. Multi-scale feature aggregated U-Net was proposed to identify membrane boundaries in intravascular ultrasound (IVUS) and it was shown that multi-scale contextual learning is crucial in identifying borders with high accuracy (1). To bring deep learning nearer to real-time clinical execution, a hardware-conscious neural architecture exploration protocol was suggested to 3D heart cine MRI segmentation by maximizing segmentation accuracy and calculational effectiveness (2). It has also considered the combination of machine learning and quantum computing systems, which have given some first indications of the development of hybrid learning-based computational models of automated design (3). Multi-exit semantic segmentation networks were suggested to allow early-exit predictions so that the computation cost can be reduced but accuracy preserved in dense prediction work (4). The development of uncertainty-sensitive accelerator modeling of computing-in-memory neural systems has enhanced neural architecture search (NAS) and hardware-sensitive modeling through supporting robust NAS in conditions of device variability (5). An on-the-fly constrained differentiable NAS architecture specifically designed to find the optimal trade-offs between quality and inference latency of segmenting 3D cardiac cine MRI images was presented (6). Besides that, a decentralized neural architecture search method based on blockchain was also described, which uses a consensus mechanism, called proof-of-neural-architecture, to facilitate collaborative and secure architecture mining (7). In 2015, a U-shaped network multi-task based was introduced to outline cardiac structures using the MRI sequences (8). An auto-weighted supervision network that uses attention mechanisms was also presented to extract myocardial scars and edema

using multi-sequence CMR images (9). The joint classification and segmentation system were offered on the basis of an interpretable multitask network, using the information bottleneck principle, to increase the model transparency and strength (10). The further improvement of the segmentation of myocardial pathology based on multi-modal cardiac MR images was made with the help of a Siamese U-Net architecture that enhanced the feature consistency across modalities (11). Lastly, a multi-sequence union-based network approach was suggested to the segmentation of myocardial pathology, which proves better generalization on various CMR inputs (12).

Other than cardiac imaging, deep learning has been applied extensively in retinal vessel segmentation. It suggested a dilated multi-scale CNN to improve the retinal vessel segmentation by obtaining long-range spatial relationships (13). An extensive comparison of the retinal vessel segmentation methods showed that deep learning-based models outperform classical ones (14). A systematic review also gave an overview of the deep learning approaches to retinal vessel segmentation with special focus on CNN-based architectures and attention (15). The use of medical image analysis in diagnostic retinopathy in diabetes has also been vastly sampled with the vessel segmentation as a main diagnostic aspect (16). The introduction of width-wise vessel bifurcation modeling later on enhanced the performance of segmentation at bifurcation points of the vessels (17).

In multimodal and cross-domain medical image segmentation, cross-modality multi-atlas segmentation was proposed to be deep registered and given a label fusion, which would allow achieving anatomical consistency between different imaging sources (18). A residual refinement network with a global-context-guided approach was suggested to the 3D cardiovascular image segmentation, which enhanced the consistency of the boundaries to a larger extent (19). Brain MRI was also subjected to CNN-based segmentation to precisely demarcate the region, which made the deep learning models versatile in neuroimaging (20). A multi-modality framework of cardiac MR images pathology segmentation proved that integrating assorted CMR sequence greatly improves the myocardial pathology detection (21). The attentive multi-view learning was realized in a hierarchical way, allowing the

direct quantification of the coronary artery stenosis on the basis of cardiac imaging data (22). Multi-level semantic adaptation was applied in few-shot learning cardiac image sequences, enabling the segmentation of cardiac sequences to be correctly performed with a small amount of labeled data (23). In smart medical systems, coronary vessels segmentation, which was based on deep learning, was used to increase the automation of the diagnosis (24). Mass segmentation in whole mammograms was also learned with attentive multi-task learning, which showed the generality of the attention-based frameworks of segmentation (25). The identification of mental diseases based on MRI images was suggested to be a 3D multi-scale CNN with attention, which supports the importance of volumetric feature learning (26).

CorLab-Net proposed anatomical dependency-aware point-cloud learning, which can be applied to automatically annotate coronary arteries, making it possible to do topology-aware vascular modeling (27). Spatial-temporal learning in X-ray angiography has also been developed on transformer-based architecture to detect coronary artery stenosis (28). An extensive review outlined the recent developments in the field of artificial intelligence in cardiac imaging with the emphasis on the role of deep learning in the segmentation, diagnosis and clinical decision support (29). Recently, a dense cascaded network was proposed to predict outliers and cardiac image segmentation, which has enhanced the resilience to noisy cardiac image inputs (30).

Medical imaging Hybrid deep learning has also been investigated (e.g. stage-wise COVID-19 classification based on X-ray images) demonstrating the flexibility of learning-based pipelines (31). A focused overview of the 10-year cardiac image segmentation on deep learning condensed the architecture trends, training methods and outstanding challenges in clinical applications (32). Traditional machine learning methods have been used in many medical and non-medical fields, such as detecting Alzheimer's disease from brain scans and checking water quality. However, these methods often struggle with complex tissue images because they depend heavily on manual feature selection and parameter tuning. To overcome these problems, modern deep

learning methods automatically learn important features from images, starting from general patterns and moving to fine details (25, 28). By combining features from different stages, these models have achieved very high accuracy, sometimes up to 98%. Other approaches divide images into small parts (patches) and make decisions based on individual patches or all patches together. Using well-known datasets, these methods have achieved accuracy levels of around 87% (31, 32).

Unsupervised learning methods, such as auto-encoders, have also been used to improve feature learning for both image and text data. Graph-based deep learning models combine relationships and structure in the data to improve predictions. Some methods further refine learning by grouping similar patterns together. Deep learning models such as DenseNet have also been successfully applied to thermal heart images for automatic heart disease detection (25, 28).

Several studies have focused on tuning model settings to improve object detection and tracking accuracy. Other deep learning models have achieved up to 95% accuracy in detecting heart diseases from MRI images (1, 2, 14, 15). Hybrid methods have been used to estimate disease severity from X-ray images. Deep learning-based segmentation techniques have been widely applied to MRI and CT scans to clearly identify and visualize body structures. Although recent methods that combine multiple image scales and learn relationships over time show promise, handling very large and complex datasets remains a major challenge (31, 32).

The proposed MultiNet framework has been used to address the cardiac classification of both binary and multiclass in a single system, which improves the flexibility and diagnostic capability. It employs the deep feature learning approach based on DenseNet201 and VGG19 and then a structured DNN-based classification head using normalization and softmax layers to achieve an accurate prediction. The model uses transfer learning, preprocessing and data augmentation to enhance robustness and alleviate overfitting. The results are systematically arranged and assessed with 70: 15: 15 train-test-validation splits and it provides evidence of the ability of the framework to analyze automated cardiac images.

## Methodology

The proposed "MultiNet" structure used in this classification is depicted in Figure 1. The starting step in this architecture is to remove the images and load the labels. Various preparation approaches are used before separating the information. The dataset size is then increased using a complex data augmentation technique. Lastly, utilizing the testing images, researchers assess the proposed "MultiNet" architecture after having trained the model separately using the HealthLNK and CAD Heart MRI Dataset.

In this study, researchers evaluate the proposed "MultiNet" framework for cardiac vascular detection using 2 publically accessible resources. The very first one gets from the Cardiac vascular Histopathological Database (HealthLNK), which would be available on the internet. This dataset consists of 7909 microscopic images of cardiac tumors, 2480 images are benign and 5429 images are deadly.

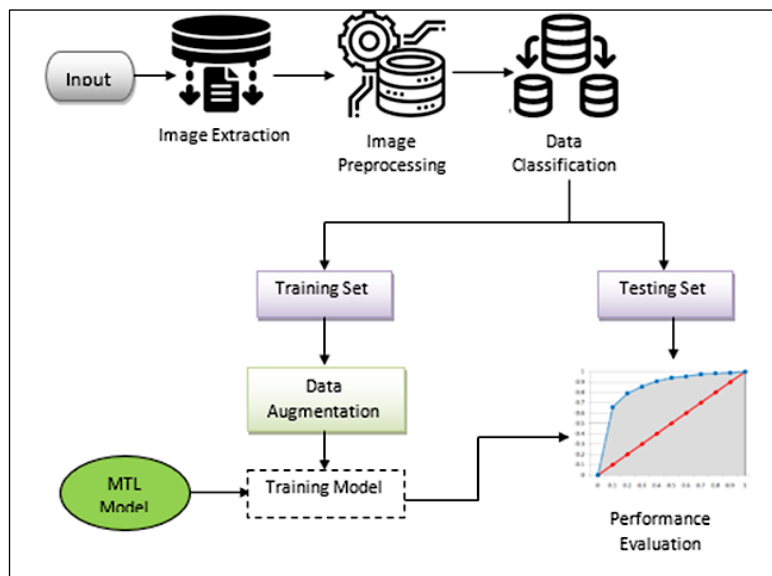


**Figure 1:** The proposed "MultiNet" Structure for Classifying Microscopic Cardiac Images

### Data-preprocessing stage

Earlier than delivering the images to the honed multi-resolution transfer teaching method, several preprocessing processes have been used. The HealthLNK dataset contains microscopic images in Portable Network Graphics (PNG) format with three channels Red, Green and Blue (RGB) and 8-bit depth for every channel. According to the transfer teaching method, researchers have lowered the photographs' original 700-460-pixel resolution of 224 x 224 pixels. To enable the system to learn more quickly and with less

resource use, humans turn each image into a numpy array. The images were then randomly jumbled so that the system could learn about certain unsorted information (32). Various data preprocessing methods work for a variety of purposes, such as expanding the dataset, addressing the over-fitting problem and strengthening the model. The data augmentation approach results in an increase of this dataset from 7909 to 54403. Table 1 contains more information about the data enhancement method.

**Table 1:** Data Augmentation Strategies

Methods	Parameter value
Zooming range	3
Rotation range	91
Shearing range	.6
Width shift range	.5
Height shift range	.5
Vertical flip	True
Horizontal flip	True

### Multi-Scale Transfer Learning Model

NASNetMobile, DenseNet-201 and VGG16 are 3 well-known CNN pre-trained systems, were combined to create the multi-scale transferable training algorithm. According to Figure 2, these algorithms segregate the low-level characteristics from the Cardiac microscopic images before

combining them with a completely connected layer for the classification problem. Improving, blurring, textures and gradient direction of the tiny images are only a few of the high-level capabilities represented by the integration of technology in education.

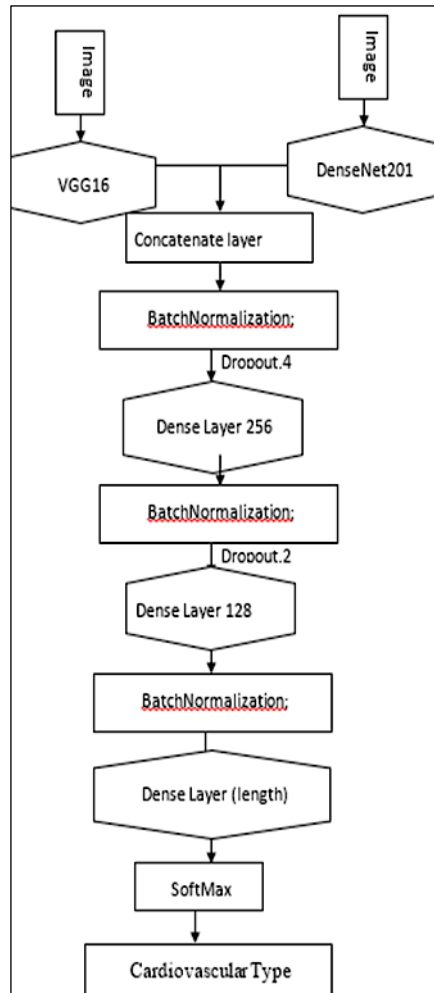


**Figure 2:** Multi-net Framework

Figure 2 demonstrates how several transferable learning methods combine for identifying Cardiac vascular categories utilizing distinct completely connected layers. All pre-trained acting as role models GlobalAveragePooling2D concurrently to smooth total layers into a course by computing the median rate of every single input channel after

features were extracted one at a time. The concatenate layers are then applied to merge every single component into a single vector. A total of 6 layers were also applied, accompanied by a softmax motivation function, to fine-tune the combined characteristics in our categorization objective, as shown in the Algorithm below.

**Algorithm**

The step by step process of Cardiac vascular segmentation and monitoring using automation presented in this section.

- Input:** Y ← One batch size (image count);
- CVD Dataset of Training - δ1;
- Dataset of Validation - δ 2;
- Dataset of Testing - δ3;

$\beta \leftarrow$  Epochs;

$\alpha \leftarrow$  Learning rate;

$\mu \leftarrow$  Batch size.

**Output:**  $\omega \leftarrow$  Pre-trained weight-CNN model

Step 1: Start

Step 2: Microscopy images converted into  $\delta 1$  with  $224 \times 224$

Step 3: Data augmentation performed to increase the size of the dataset.

Step 4: Features extracted from microscopy images from pre-trained models through using NasNetMobile; DenseNet-201 and VGG16 CNN.

Step 5: Concatenate layer merge the extracted features

Step 6: Fine-tuned layers set with CNN<sub>batchnormalization</sub>, CNN<sub>dense</sub> CNN<sub>softmax</sub> CNN<sub>dropout</sub>,

Step 7: Pre-trained model initializes the parameters such as  $\alpha, \beta, \mu, \gamma$ .

Step 8: "MultiNet" framework trained to determine the weights at initial stage

Step 9: for  $\beta$  ranges from 1 to  $\beta$  do

{Step 9.1: Select  $\gamma$  for  $\delta 1$ .

Step 9.2: Determine the loss function using back propagation

Step 9.3: update the weight  $\omega$  through back propagation}

The VGGNet structure outperformed the Alex Net design, with a failure rate of only 8.1%. There are 5 levels in the convolution operation. The use of the ReLU purpose as a non-linear kernel method ensures that output for every thorough level is more potent in every succeeding max-pooling tier. The next five levels have depths of 64, 128, 256,

512 and 512, respectively. The trainable variables are reduced by max-pooling in every one of the subspaces that make up every tier. The extracted features of the proposed VGG19 models were obtained using a crucial rule that was enforced in the final stage. Figure 3 provides a detailed representation of the VGG19-based CNN model.

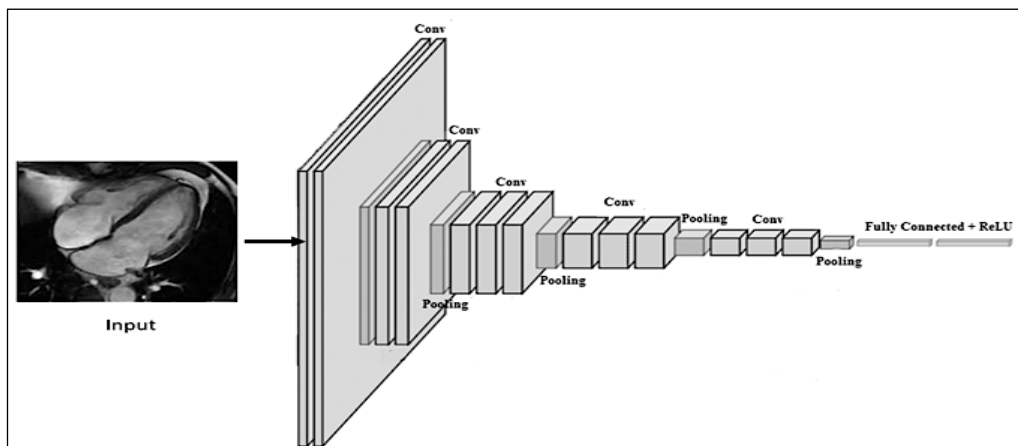


**Figure 3:** VGG19-based CNN Architecture

From a research point of view, this study improves how computers analyze heart images by fixing problems found in methods that use only one deep learning model. Earlier methods usually depend on a single neural network, which often struggles to correctly understand complex heart tissue shapes, especially when the data comes from different sources or includes multiple disease types. This can lead to confusion between classes and unreliable results.

To solve these issues, this study introduces a MultiNet approach, where several well-trained

deep learning models work together instead of relying on just one. Each model learns different types of information from the heart images, such as shapes, patterns and textures. These features are then combined early in the process, allowing the system to make more accurate and confident decisions. This is different from older methods that simply combine final predictions without deeply understanding the image features. Another important strength of the proposed method is that it can handle both simple two-class problems (such as healthy vs. diseased) and more complex multi-

class problems within the same system. Many existing studies focus on only one type of classification, which limits their usefulness in real clinical settings. The use of a well-structured neural network with proper normalization helps the model learn smoothly and perform consistently across different heart disease categories. Overall, this research introduces a flexible and scalable learning strategy that can be applied not only to heart images but also to other medical imaging tasks. The improved accuracy and reliability show that the MultiNet approach has strong potential to support doctors by providing faster, more dependable computer-assisted diagnosis, helping bridge the gap between research models and real-world clinical use.

Despite the promising performance of the proposed MultiNet-based cardiac classification framework, several limitations of the present study should be acknowledged. Second, the proposed framework relies on pre-trained convolutional neural networks, which increases computational complexity and inference time. Additionally, the study does not explicitly address

model interpretability, which is an important requirement for clinical acceptance and trust in AI-assisted diagnostic systems.

### Experimental Setup

The CAD Cardiac MRI Dataset and HealthLNK's "Multi-Net" architecture was used in the research, together with the experimental set - up, model parameters and outcomes. An accurate contrast between proposed access and various CNN pre-trained architectures is also covered. An open-source package called Keras was used to create the proposed "MultiNet" architecture because it connected Python with the human brain.

### Performance Metrics

The effectiveness of the proposed framework is assessed using a variety of statistical metrics, such as Accuracy, Recall, Precision (Equation [1]), False-Positive Rate (FPR) (Equation [2]), True Negative Rate (TNR) (Equation [3]), F1-score (Equation [4]), Kappa Statistical (Equation [5]) and Matthews Correlation Coefficient (MCC) (Equation [6]). These characteristics, which include True Positive ( $T_P$ ); False Positive ( $F_P$ ), True Negative ( $T_N$ ) and False Negative ( $F_N$ ) were based on results for the contingency table.

$$\text{Precision (Pr)} = \frac{T_P}{T_P + F_P} \quad [1]$$

$$\text{FPR} = \frac{F_P}{F_P + T_N} \quad [2]$$

$$\text{TNR} = \frac{T_N}{T_N + F_P} \quad [3]$$

$$\text{F1 - score} = 2 \times \frac{\text{Pr} \times \text{Re}}{\text{Pr} + \text{Re}} \quad [4]$$

$$\text{Kappa} = \frac{\text{Total Accuracy} - \text{Random Accuracy}}{1 - \text{Random Accuracy}} \quad [5]$$

$$\text{MCC} = \frac{T_P \times T_N - F_P \times F_N}{\sqrt{(T_P + F_P)(T_N + F_P)(T_P + F_N)(T_N + F_N)}} \quad [6]$$

## Results and Discussion

Figures 4(A) and 4(B) shows a simulated result of the learning proposed "MultiNet" architecture using the HealthLNK dataset. Values for the hyper-parameters used to train frameworks were shown in Table 2. The planner value and also the gradient descent transfer functions are two important hyper-parameters for training a model. Since Adam includes the essential characteristics of the AdaGrad and RMSProp optimizers and it can

manage patchy gradients on a big dataset, researchers select adam as an optimization algorithm. The research depends on a categorization model for the HealthLNK sets of data, select double log loss as an error purpose. We need a number for the appropriate training level to minimize the loss of function. Choosing an information gain is difficult, though having an educated rate results in inappropriate behavior.

Small learning rates result in longer conditioning workouts and sparse weight updates even by model. In this study, researchers select a learning rate of 0.0001 to prevent such problems. A reasonable generalization of the model may be

seen by the usage of the minimum batch level for 32. The proposed framework received 50th epoch training. Furthermore, the models only reached more than 97 after the 29th training period.

**Table 2:** "MultiNet" Parameter

Dataset size	Parameter Methods	Value
HealthLKNK	Optimization	Adam
	Learning rate	.0002
	Loss Function value	Binary_crossentropy
	Performance metrcks	Accuracy
	Batch (Size)	33
	Epoc	52
ICIAR	Optimization	Adam
	Learning rate	.0002
	Loss Function value	categorical_crossentropy
	Performance metrcks	Accuracy
	Batch (Size)	33
	Epochs	198

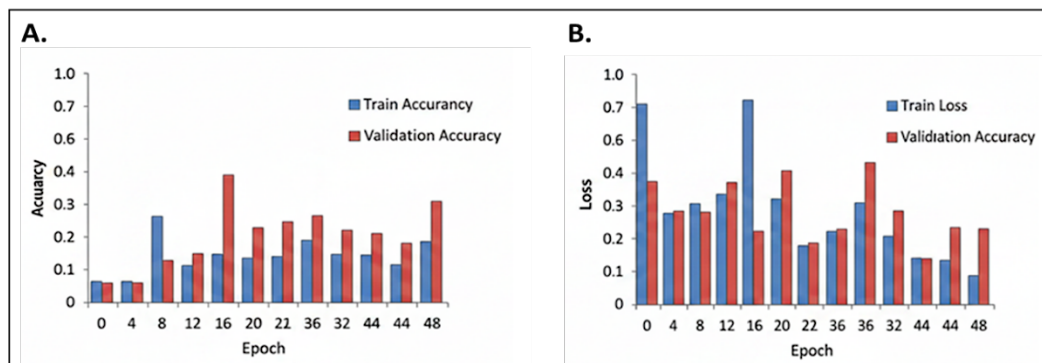


**Figure 4:** HealthLKNK Dataset: A. Calibration and Testing Correctness (Greater is Preferable), B. Learning and Validation Loss (Lower is Better)

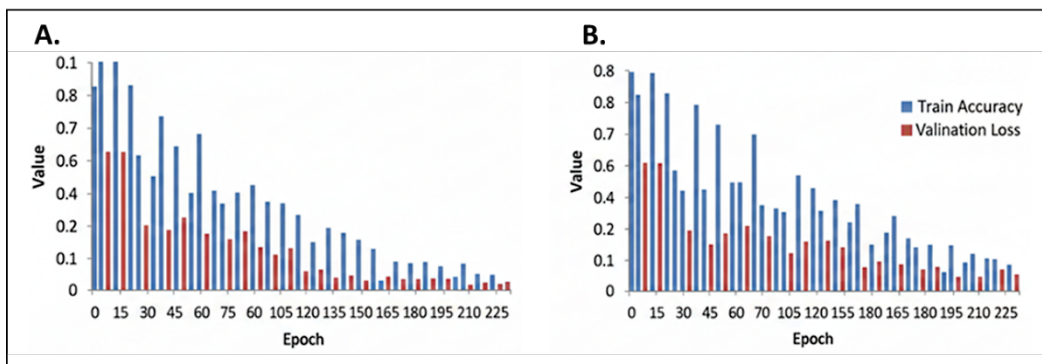


**Figure 5:** ICIAR Dataset: A. Calibration and Testing Accuracy (Greater is Preferable), B. Learning and Validation Loss (Lower is Better)

During learning with the proposed "MultiNet" architecture, quality improvement and loss are shown for the CAD Cardiac MRI Dataset in Figure 5 (A). Table 2 displays the hyper-parameter settings used to train the system. Already our research depends on the categorization tasks for the CAD Cardiac MRI set of data select a category cross-

entropy as an error function. Due to the small number of images in this collection, the proposed method required to be additional training following the 166th epoch, the "MultiNet" structure had learned for 200 epochs and learning rate had reached 95%. Thus, throughout the validation stage, the total accuracy rate was 94.4

percent. Moreover, it is evident from the error function curve in Figure 5(B) that there aren't any fluctuations and also the loss value is nearly zero. Figures 6(A) and 6(B) displays Confusion matrix and ROC curves for the HealthLNK sample using the "CardiacMultiNet" structure. DenseNet201 and VGG19 2 well-known domain adaptation techniques were combined in the proposed model, which employed the fusion features to assess whether heart muscle was malignant or benign. Figure 6(A) demonstrates that all but one of the images were appropriately identified as benign and cancerous Cardiac carcinoma. The proposed approach concurrently misclassifies merely one harmless microscopic image. The region rating for

this strategy was 0.998, indicating consistency and dependability in the system. To further comprehend the utility of the "CardiacMultiNet" structure, multiple deep learning approaches were separately evaluated on the HealthLNK information. The "CardiacMultiNet" structures along with the other different transfer learning models are contrasted in Table 3. The "CardiacMultiNet" structure outperforms all currently used modern systems utilizing overall accuracy; Recall, F1-score and MCC of 0.997, 0.995 and 993. The system was successful as evidenced by an FNR of 0.010 and also a TNR is relatively almost just one.

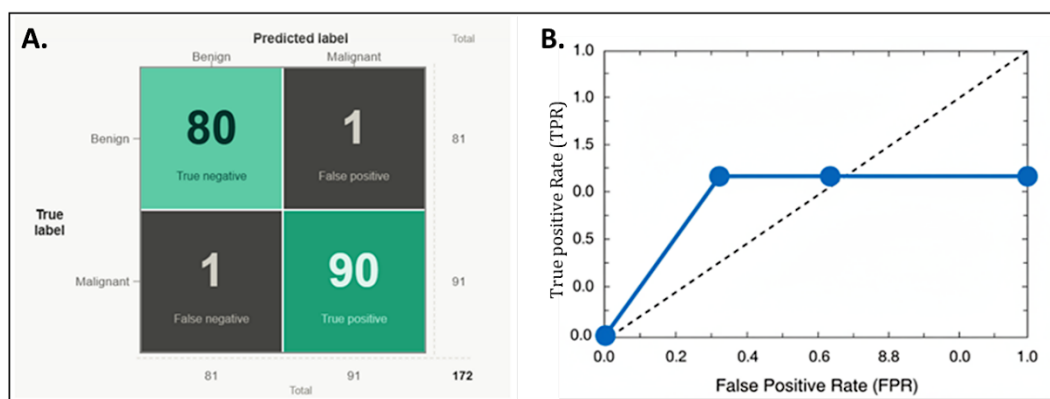


**Figure 6:** The Different Classifiers: A. HealthLNK Dataset, B. ROC Curve

Table 3 presents a comparative performance analysis of DenseNet201, VGG19 and the proposed method for cardiac image classification across benign and malignant classes. Among the evaluated approaches, the proposed method demonstrates consistently superior performance across all statistical metrics. DenseNet201 achieves strong baseline results, with average precision, recall and F1-score values of 0.947, 0.946 and 0.953, respectively. Its FPR remains relatively low, indicating reliable discrimination; however, the presence of moderate false positives and false negatives limits its overall robustness, as reflected by an average MCC of 0.907. The VGG19 model performs worse compared to the other methods, especially when it comes to correctly identifying diseased cases and maintaining reliable predictions. It makes more false alarms for malignant cases, which lowers its ability to correctly recognize healthy samples and reduces its overall reliability. Because of this, its overall performance score is lower, showing that VGG19 struggles to properly handle differences between

heart image classes. On the other hand, the proposed method makes very few mistakes for both benign and malignant cases. It correctly identifies almost all samples, resulting in very high accuracy and consistency. The number of false detections is extremely low and the model achieves nearly perfect scores across key performance measures. This shows that the proposed method produces highly dependable results, even when the dataset has an unequal number of samples in each class. Overall, these findings clearly show that the proposed method is more accurate, stable and trustworthy than existing deep learning models for classifying cardiac images. The excellent performance of the proposed CardiacMultiNet framework on the HealthLNK dataset is in line with recent reports that multi-feature and deep ensemble strategies have been found to demonstrate greater robustness (compared to single-network models) in cardiac MRI and medical image analysis literature. Indicatively, automated cardiac MRI segmentation methods that utilize deep learning

have shown that using more detailed representations of features enhances delineation and diagnostic accuracy of more complex cardiac structures (1,5). On the same note, current research works have also indicated that adaptive and hybrid segmentation/classification models are more effective than traditional CNN pipelines in that they utilize features more effectively, show spatial consistency and distinguish fine pathological structures (14, 26, 27). Compared to these previous reports, the suggested approach

learns with extremely high classification accuracy and low false positive, which confirms the fact that early feature fusion between multiple pre-trained networks, can better represent inter-class variability, rather than simply using a single backbone network. This observation also aligns with the recent reviews that provide benefits of hybrid and multi-scale deep learning frameworks in cardiac image detection, particularly where complexity and visual diversity of the dataset are challenging (25, 28, 31).

**Table 3:** Comparison of "CardiacMultiNet" approach and methods on HealthLNK collection

Method	Cardiac type	TP	TN	FP	FN	Pre	Re	FPR	TNR	F1-score	MCC
DensNet201	Benign					0.944	0.957	0.046	0.946	0.951	0.907
	Malignant	73	82	5	4	0.959	0.946	0.040	0.956	0.958	0.909
	Average Score	82	73	4	5	0.947	0.946	0.037	0.957	0.953	0.907
VGG19	Benign					0.947	0.917	0.040	0.957	0.932	0.875
	Malignant	70	82	5	7	0.927	0.952	0.082	0.921	0.937	0.868
	Average Score	82	70	7	5	0.936	0.936	0.056	0.937	0.936	0.867
Proposed Method	Benign					0.989	0.989	0.012	0.90	0.990	0.978
	Malignant	80	90	2	2	0.990	0.990	0.013	0.989	0.995	0.991
	Average Score	90	80	2	2	0.990	0.990	0.012	0.990	0.993	0.985

Note: TP – True Positive, TN – True Negative, FP – False Positive, FN – False Negative, Pre – Precision, Re – Recall, FPR – False Positive Rate, TNR – True Negative Rate, MCC – Matthews Correlation Coefficient.

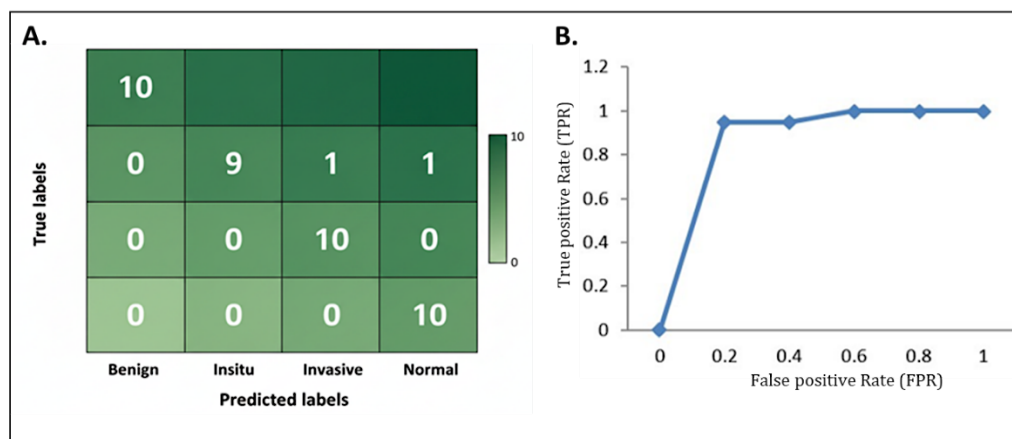


**Figure 7:** The Different Classifiers: A. ICIAR Dataset, B. ROC Curve

Figure 7 illustrates the uncertainty sequences and ROC area for the ICIAR sample that use the "CardiacMultiNet" framework. In this collection, the concept approach acknowledges the multi-class classification carcinoma group, which includes such as invasive, normal and benign carcinomas. The correct classification of the microscope images 10, 8, 10 and 10 as 4 different forms of multiple tumors is shown in Figure 7(A). On the other side, the "CardiacMultiNet" architecture misclassifies merely one harmless

microscopic image. The surface rating for this model is 0.935, indicating that it has been informative and regular in Figure 7(B). The "CardiacMultiNet" structure produces Accuracy 0.995, Recall 0.996, MCC and F1-score of 0.991 according to a comparative evaluation included in Table 4. Table 4 demonstrates that, in terms of determining Cardiac vascular subtypes, the framework fared higher than the other two approaches.

**Table 4:** Comparison of "CardiacMultiNet" Approach and Methods on ICIAR Collection

Method	Cardiac type	TP	TN	FP	FN	Pre	Re	FPR	TNR	F1-score	MCC
DenseNet201	Benign	11	29	3	0	0.832	1.000	0.056	0.946	0.911	0.882
	In-situ	9	31	0	3	1.000	0.804	0.000	1.000	0.895	0.874
	Normal	9	30	2	3	0.893	0.803	0.030	0.969	0.843	0.795
	Invasive	10	29	3	2	0.819	0.903	0.057	0.939	0.857	0.813
VGG19	Benign	8	26	6	4	0.585	0.704	0.157	0.836	0.636	0.504
	In-situ	5	30	2	7	0.803	0.397	0.027	0.973	0.527	0.485
	Normal	10	26	6	2	0.637	0.902	0.163	0.845	0.745	0.667
	Invasive	7	28	4	5	0.675	0.602	0.103	0.905	0.632	0.527
Proposed Method	Benign	11	31	0	0	1.000	1.000	0.000	1.000	1.000	1.000
	In-situ	9	31	0	3	1.000	0.801	0.000	1.000	0.892	0.872
	Normal	11	30	2	0	0.911	1.000	0.034	0.971	0.954	0.941
	Invasive	11	30	2	0	0.911	1.000	0.034	0.971	0.954	0.941
	Average Score					0.962	0.952	0.019	0.991	0.953	0.942

**Note:** TP – True Positive, TN – True Negative, FP – False Positive, FN – False Negative, Pre – Precision, Re – Recall, FPR – False Positive Rate, TNR – True Negative Rate, MCC – Matthews Correlation Coefficient.

Table 4 summarizes the multi-class classification performance of DenseNet201, VGG19 and the proposed method across four cardiac histopathological categories: benign, in-situ, normal and invasive. Overall, the proposed method consistently outperforms the baseline deep learning models in terms of accuracy, robustness and class-wise reliability. DenseNet201 demonstrates moderate and relatively balanced performance across classes, with precision values ranging from 0.819 to 1.000 and recall values between 0.803 and 1.000. While the model achieves low false positive rates, particularly for the in-situ class, its performance degrades for normal and invasive cases, as reflected by reduced F1-scores and MCC values. This indicates limitations in capturing subtle inter-class variations in complex histopathological patterns. VGG19 exhibits the weakest performance among the three methods. It shows noticeable variability across classes, with low precision and recall for benign and in-situ categories. The higher false positive rates and lower MCC values suggest reduced discriminative capability and instability in multi-class decision making, particularly when class boundaries are less distinct. In contrast, the proposed method achieves near-optimal results across all four classes. It records perfect or near-perfect precision and recall for benign, normal and invasive categories, with zero or minimal false positives and false negatives. The low average false positive rate (0.019), high true negative rate (0.991) and superior average F1-score (0.953) and

MCC (0.942) confirm the robustness and generalization capability of the proposed approach. These results demonstrate that the proposed method effectively handles inter-class variability and complexity, making it well-suited for reliable multi-class cardiac image classification. The multi-class findings also support the efficacy of the proposed framework to manage class boundaries, which are more difficult. This matters to the extent that other past studies in the domain of cardiac and multimodal medical imaging have observed that performance tends to decline when models are needed to identify multiple subtypes of pathology, instead of making binary distinctions (3, 9, 12). Recent studies of multi-modality and pathology-minded segmentation also claimed that high and strong multi-class performance requires combination of complementary features and better contextual learning (11, 12, 18). Consequently, according to such results, the proposed approach has a high precision, recall and MCC values in a range of categories, implying that the integrated DenseNet-VGG feature representation has a higher ability to separate classes than the separate transfer learning models. The findings are hence consistent with the emerging body of evidence which positively suggest that the combination of intertwined deep representations and multi-scale learning strategy may lead to improved generalization in complex medical image classification tasks (15, 26).

All in all, the experimental results show that CardiacMultiNet provides a more consistent and

precise solution when compared to single transfer learning models both in binary and multi-class cardiac image recognition. This improvement could be explained by the combination of complementary deep features, which assists the framework to pick fine structural and textural variations that otherwise might be overlooked by an individual architecture. This finding can be compared to the previous research which reveals that multi-network, multi-scale and hybrid deep learning designs outperform standalone CNN models in their cardiac MRI segmentation and diagnostic related tasks (2, 6, 14, 27, 30). Moreover, recent studies have stressed the fact that a powerful automated cardiac image processing procedure should not only have a high accuracy but also consistency under a wide variety of pathological patterns and imaging conditions (4, 25, 31). In this light it is possible to say that the current findings indicate the practical potential of the proposed framework in the computer-aided diagnosis. Nevertheless, the computational complexity of several pre-trained backbones and the inability to interpret them are also significant drawbacks and the future research should include lightweight design, explainable AI consideration and test on larger multi-centers.

## Conclusion

This study presented CardiacMultiNet, a robust deep learning framework for cardiac image classification using complementary feature learning from multiple pre-trained CNN models. The framework demonstrated strong and consistent performance on both binary and multi-class tasks, indicating its ability to effectively distinguish complex cardiac image patterns. The experimental results show that the proposed method improves classification reliability when compared with individual deep learning models, particularly in challenging categories. These findings suggest that CardiacMultiNet can serve as a useful computer-aided diagnostic support tool for cardiac image analysis. In future work, the model can be extended through validation on larger multi-center datasets, incorporation of explainable AI techniques and optimization for faster clinical deployment.

The results show that CardiacMultiNet performs better than individual deep learning models. It achieved very high accuracy up to 95% and 99%

on the HealthLNK dataset. Most importantly, the model is especially good at identifying malignant (cancerous) heart images, which is crucial for early detection and timely treatment. These findings suggest that CardiacMultiNet can serve as a dependable computer-based support system for doctors. It can help them diagnose heart cancer more quickly and accurately, which may improve patient outcomes and survival rates. In the future, the model will be tested on larger datasets collected from multiple hospitals to ensure it works well in real clinical environments. The researchers also plan to add explanation tools that show why the model makes certain decisions, helping doctors trust and understand the results. Additionally, efforts will be made to make the system faster and more efficient and to include other types of patient information like clinical records and imaging details to further improve its usefulness in real-world medical practice.

## Abbreviations

AUC: area under the receiver operating characteristic curve, CMR: cardiac magnetic resonance, CNN: convolutional neural network, DNN: deep neural network, F1: F1-score, FN: false negative, FP: false positive, IoU: intersection over union, MCC: Matthew's correlation coefficient, MRI: magnetic resonance imaging.

## Acknowledgement

The authors would like to acknowledge the support of their institution and colleagues who provided guidance during the research process. Special thanks are extended to the technical staff for their assistance with data preparation and analysis. The authors also acknowledge the reviewers of IRJMS for their valuable feedback, which significantly improved the quality and presentation of this manuscript.

## Author Contributions

Muthuraja M: conceptualization, methodology design, implementation of the models, experiments, data analysis, manuscript drafting, Rasmi A: conceptualization, methodology design, implementation of the models, experiments, data analysis, manuscript drafting, Shanmuga Priya S: conceptualization, methodology design, implementation of the models, experiments, data analysis, manuscript drafting, Maheswari K: conceptualization, methodology design, imple-

mentation of the models, experiments, data analysis, manuscript drafting, Nandhagopal Subramani: experiments, data analysis, critical review, editing of the manuscript, Aravindhraj N: supervision, validation of results, Sherubha P: supervision, validation of results. All the authors have read and approved the final version of the manuscript.

### Conflict of Interest

The authors declare no conflict of interest.

### Data Availability

The data that support the findings of this study are available from the corresponding author upon reasonable request.

### Declaration of Artificial Intelligence (AI) Assistance

Generative AI tools (such as ChatGPT) were used to assist in language refinement, rephrasing for clarity, checking grammar and supporting reference research during the preparation of this manuscript. All references included were verified by the authors from original sources before citation. The authors confirm that all content, analysis and conclusions were developed by the authors themselves, who reviewed and approved every section. The authors take full responsibility for the integrity and accuracy of the final version of the manuscript.

### Ethics Approval

Not applicable. This study used publicly available, de identified datasets [e.g., ACDC, WHS, MAS]; no human subjects were directly involved and no identifiable personal data were used. If applicable, replace with: "The study protocol was approved by the Institutional Ethics Committee, approval number and conducted in accordance with the Declaration of Helsinki."

### Funding

The author(s) received no financial support for the research, authorship and/or publication of this article.

### References

1. Chai WY, Lin G, Wang CJ, *et al.* A deep learning-based fully automated cardiac MRI segmentation approach for Tetralogy of Fallot patients. *J Magn Reson Imaging.* 2026;63(1):264–276. doi:10.1002/jmri.70113
2. Paciorek AM, von Schacky CE, Foreman SC, *et al.* Automated assessment of cardiac pathologies on cardiac MRI using T1-mapping and late gadolinium phase sensitive inversion recovery sequences with deep learning. *BMC Med Imaging.* 2024;24(1):43. doi:10.1186/s12880-024-01217-4
3. Jafari R, Verma R, Aggarwal V, Gupta RK, Singh A. Deep learning-based segmentation of left ventricular myocardium on dynamic contrast-enhanced MRI: a comprehensive evaluation across temporal frames. *Int J Comput Assist Radiol Surg.* 2024;19(10):2055–2062. doi:10.1007/s11548-024-03221-z
4. Yao T, St Clair N, Miller GF, *et al.* A deep learning pipeline for assessing ventricular volumes from a cardiac MRI registry of patients with single ventricle physiology. *Radiol Artif Intell.* 2024;6(1):e230132. doi:10.1148/ryai.230132
5. Sun X, Cheng LH, Plein S, Garg P, van der Geest RJ. Deep learning based automated left ventricle segmentation and flow quantification in 4D flow cardiac MRI. *J Cardiovasc Magn Reson.* 2024;26(1):100003. doi:10.1016/j.jocmr.2023.100003
6. Lu Q, Xu X, Dong S, *et al.* RT-DNAS: real-time constrained differentiable neural architecture search for 3D cardiac cine MRI segmentation. In: *MICCAI 2022, Part V.* Cham: Springer; 2022. p. 602–612. doi:10.1007/978-3-031-16443-9\_58
7. Chai WY, Lin G, Wang CJ, Chiang HJ, Ng SH, Kuo YS, Lin YC. A Deep Learning-Based Fully Automated Cardiac MRI Segmentation Approach for Tetralogy of Fallot Patients. *J Magn Reson Imaging.* 2026 Jan;63(1):264-276. doi: 10.1002/jmri.70113
8. Li W, Wang L, Qin S. CMS-UNet: cardiac multi-task segmentation in MRI with a U-shaped network. In: *MyoPS 2020 Proceedings.* Cham: Springer; 2020: 92–101. doi:10.1007/978-3-030-65651-5\_9
9. Wang KN, Yang X, Miao J, *et al.* AWSnet: an auto-weighted supervision attention network for myocardial scar and edema segmentation in multi-sequence cardiac magnetic resonance images. *Med Image Anal.* 2022;77:102362. doi:10.1016/j.media.2022.102362
10. Wang J, Zheng Y, Ma J, *et al.* Information bottleneck-based interpretable multitask network for breast cancer classification and segmentation. *Med Image Anal.* 2023;83:102687. doi:10.1016/j.media.2022.102687
11. Li W, Wang L, Li F, Qin S, Xiao B. Myocardial pathology segmentation of multi-modal cardiac MR images with a simple but efficient Siamese U-shaped network. *Biomed Signal Process Control.* 2022;71:103174. doi:10.1016/j.bspc.2021.103174
12. Qiu J, Li L, Wang S, *et al.* MyoPS-Net: myocardial pathology segmentation with flexible combination of multi-sequence CMR images. *Med Image Anal.* 2023;84:102694. doi:10.1016/j.media.2022.102694
13. Pan N, Li Z, Xu C, Gao J, Hu H. Hybrid method for automatic initialization and segmentation of ventricular on large-scale cardiovascular magnetic

- resonance images. *BMC Med Imaging*. 2025;25(1): 155.  
doi:10.1186/s12880-025-01683-4
14. Popescu AB, Seitz A, Becker M, Mahrholdt H, Wetzl J, Jacob A, et al. Deep learning-based segmentation of T1 and T2 cardiac MRI maps for automated disease detection. *Eur Radiol*. 2025.  
doi:10.1007/s00330-025-12069-z
  15. Xu W, Shi J, Lin Y, et al. Deep learning-based image segmentation model using an MRI-based convolutional neural network for physiological evaluation of the heart. *Front Physiol*. 2023;14: 1148717.  
doi:10.3389/fphys.2023.1148717
  16. Wu B, Fang Y, Lai X. Left ventricle automatic segmentation in cardiac MRI using a combined CNN and U-net approach. *Comput Med Imaging Graph*. 2020;82:101719.  
doi:10.1016/j.compmedimag.2020.101719
  17. Liu F, Wang K, Liu D, Yang X, Tian J. Deep pyramid local attention neural network for cardiac structure segmentation in two-dimensional echocardiography. *Med Image Anal*. 2021;67: 101873.  
doi:10.1016/j.media.2020.101873
  18. Ding W, Li L, Zhuang X, Huang L. Cross-modality multi-atlas segmentation via deep registration and label fusion. *IEEE J Biomed Health Inform*. 2022;26(7):3104–3115.  
doi:10.1109/JBHI.2022.3149114
  19. Liu J, Wei A, Guo Z, Tang C. Global context and enhanced feature guided residual refinement network for 3D cardiovascular image segmentation. *IEEE Access*. 2021;9:155861–155870.  
doi:10.1109/ACCESS.2021.3129333
  20. Moafi A, Moafi D, Mirkes EM, et al. Robust deep learning for myocardial scar segmentation in cardiac MRI with noisy labels. In: *MICCAI 2025 Proceedings*. Cham: Springer; 2026: 529–539. doi:10.1007/978-3-032-05169-1\_51
  21. Zhang Z, Liu C, Ding W, et al. Multi-modality pathology segmentation framework: application to cardiac magnetic resonance images. In: *MyoPS 2020 Proceedings*. Cham: Springer; 2020: 37–48.  
doi:10.1007/978-3-030-65651-5\_4
  22. Zhang D, Yang G, Zhao S, et al. Direct quantification of coronary artery stenosis through hierarchical attentive multi-view learning. *IEEE Trans Med Imaging*. 2020;39(12):4322–4334.  
doi:10.1109/TMI.2020.3017275
  23. Guo S, Xu L, Feng C, Xiong H, Gao Z, Zhang H. Multi-level semantic adaptation for few-shot segmentation on cardiac image sequences. *Med Image Anal*. 2021;73:102170.  
doi:10.1016/j.media.2021.102170
  24. Xian Z, Wang X, Yan S, Yang D, Chen J, Peng C. Main coronary vessel segmentation using deep learning in smart medical. *Math Probl Eng*. 2020;2020: 8858344.  
doi:10.1155/2020/8858344
  25. Zhou C, Dai P, Hou A, et al. A comprehensive review of deep learning-based models for heart disease prediction. *Artif Intell Rev*. 2024;57(10):263.  
doi:10.1007/s10462-024-10899-9
  26. Elizar E, Muharar R, Zulkifley MA. DeSPNet: A multiscale deep learning model for cardiac segmentation. *Diagnostics (Basel)*. 2024;14(24): 2820.  
doi:10.3390/diagnostics14242820
  27. Aghapanah H, Rasti R, Kermani S, et al. CardSegNet: An adaptive hybrid CNN-vision transformer model for heart region segmentation in cardiac MRI. *Comput Med Imaging Graph*. 2024;115:102382.  
doi:10.1016/j.compmedimag.2024.102382
  28. Yang G, Zhang H, Firmin D, Li S. Recent advances in artificial intelligence for cardiac imaging. *Comput Med Imaging Graph*. 2021;90:101928.  
doi:10.1016/j.compmedimag.2021.101928
  29. Rasmi A, Jayanthiladevi A, Sunitha HD. A dense cascaded network model for outlier prediction and segmentation of cardiac images. *Int J Intell Syst Appl Eng*. 2024;12(13s):302–308.  
<https://ijisae.org/index.php/IJISAE/article/view/4597/3268>
  30. Schwab M, Pamminger M, Kremser C, Haltmeier M, Mayr A. Deep learning pipeline for fully automated myocardial infarct segmentation from clinical cardiac MR scans. *Radiol Adv*. 2025;2(4):umaf023.  
doi:10.1093/radadv/umaf023
  31. Chen S, Qiu C, Yang W, Zhang Z. Multiresolution aggregation transformer UNet based on multiscale input and coordinate attention for medical image segmentation. *Sensors (Basel)*. 2022;22(10):3820.  
doi:10.3390/s22103820
  32. Qi Y, Hu C, Zuo L, Yang B, Lv Y. Cardiac magnetic resonance image segmentation method based on multi-scale feature fusion and sequence relationship learning. *Sensors (Basel)*. 2023;23(2): 690.  
doi:10.3390/s23020690

**How to Cite:** Muthuraja M, Rasmi A, Priya SS, Maheswari K, Subramani N, Aravindhraj N, Sherubha P. CardiacMultiNet: Learning Model for Segmenting the Cardiac Images in Magnetic Resonance. *Int Res J Multidiscip Scope*. 2026; 7(2): 1630-1643. DOI: 10.47857/irjms.2026.v07i02.07411